



Substituted thiobenzoic acid *S*-benzyl esters as potential inhibitors of a snake venom phospholipase A₂: Synthesis, spectroscopic and computational studies

I.C. Henao Castañeda^{a,*}, J.A. Pereañez^{a,b}, J.L. Jios^c

^a Programa de Ofidismo y Escorpionismo, Departamento de Farmacia, Facultad de Química Farmacéutica, Universidad de Antioquia, Calle 67, No. 53 108, Apartado Aéreo 1226, Medellín, Colombia

^b Facultad de Medicina, Universidad Cooperativa de Colombia, Medellín-Colombia, Calle 48 # 28-00, Medellín, Colombia

^c Unidad LaSeSiC-PlaPiMu, Departamento de Química, Facultad de Ciencias Exactas, Universidad Nacional de La Plata, 47 esq. 115, 1900 La Plata, Argentina

HIGHLIGHTS

- ▶ Substituted thiobenzoic acid *S*-benzyl esters were synthesized and characterized.
- ▶ Thioesters inhibited the enzymatic activity of a venom phospholipase A₂.
- ▶ Molecular docking study suggests that compounds could interact with His48 at the active site of PLA₂.
- ▶ Further *in vivo* studies are required to confirm the antiophidic potential of thioesters.

ARTICLE INFO

Article history:

Received 2 May 2012

Received in revised form 13 June 2012

Accepted 14 June 2012

Available online 20 June 2012

Keywords:

Thioesters
Phospholipase A₂
Docking
Snake venom
DFT calculations
Conformational analysis

ABSTRACT

4-Chlorothiobenzoic acid *S*-benzyl ester (**I**), 3-nitrothiobenzoic acid *S*-benzyl ester (**II**), 4-nitrothiobenzoic acid *S*-benzyl ester (**III**) and 4-methylthiobenzoic acid *S*-benzyl ester (**IV**) were prepared and characterized by ¹H and ¹³C NMR, Mass spectrometry and IR spectroscopy. Quantum chemical calculations were performed with Gaussian 09 to calculate the geometric parameters and vibrational spectra. Phospholipase A₂ (PLA₂) was purified from *Crotalus durissus cumanensis* venom by molecular exclusion chromatography, followed by reverse phase-high performance liquid chromatography. Two studies of the inhibition of phospholipase A₂ activity were performed using phosphatidilcholine and 4-nitro-3-octanoyloxybenzoic acid as substrates, in both cases compound **II** showed the best inhibitory ability, with 74.89% and 69.91% of inhibition, respectively. Average percentage of inhibition was 52.49%. Molecular docking was carried out with Autodock Vina using as ligands the minimized structures of compounds (**I–IV**) and as protein PLA₂ (PDB code 2QOG). The results suggest that compounds **I–IV** could interact with His48 at the active site of PLA₂. In addition, all compounds showed Van der Waals interactions with residues from hydrophobic channel of the enzyme. This interaction would impede normal catalysis cycle of the PLA₂.

© 2012 Elsevier B.V. All rights reserved.

1. Introduction

Snakebites represent a relevant public health issue in many regions of the world, particularly in tropical and subtropical countries of Africa, Asia, Latin America and Oceania [1]. The pathophysiological effects observed in ophidian bites combine the action of several enzymes, proteins and peptides, which include phospholipases A₂, hemorrhagic metalloproteases and other proteolytic enzymes, coagulant components, neurotoxins, cytotoxins and cardiotoxins, among others [2]. Phospholipases A₂ (PLA₂; EC 3.1.1.4) are enzymes that abundantly occur in snake venoms with crucial action in the hydrolysis of phospholipids. PLA₂ can also

induce several pharmacological effects such as edema, modulation of platelet aggregation, as well as neurotoxic, anticoagulant and myotoxic effects [3,4].

The structure of PLA₂s is composed of three long helices (two of them are antiparallel), two antiparallel β sheets and a calcium-binding loop. These proteins have a variable length from 119 to 134 amino acids. Their antiparallel α helices (residues 37–57 and 90–109, respectively) together with the N-terminal helix (residues 1–12), define the hydrophobic channel. This structure leads the substrate to the active site, which is formed of four residues: His48, Asp49, Tyr52 and Asp99. Asp49 in combination with Tyr28, Gly30 and Gly32 form the calcium-binding loop, which is responsible for coordinating the Ca²⁺ required during catalysis [5]. In addition, there is an interfacial binding surface, which mediates the adsorption of the enzyme onto the lipid–water interface of

* Corresponding author. Tel.: +57 4 2195476.

E-mail address: ihenao@farmacia.udea.edu.co (I.C. Henao Castañeda).

the phospholipid membrane bilayer. These general features are common to both groups I and II of PLA₂s, which mainly differ in the position of one of their seven disulfide bonds [5].

Myonecrosis is a common finding in snakebites, which is caused by PLA₂, one of the most important and abundant muscle damaging components present in snake venoms. The action of these enzymes over membrane phospholipids includes the release of fatty acids such arachidonic acid, which is a precursor of pro-inflammatory eicosanoids [6]; moreover, such degradation, can lead to destabilization of the phospholipids bilayer [4].

The therapy of snakebite has been based on the intravenous administration of equine or ovine antivenoms [4]. However, it has been demonstrated that this therapy generally has a limited efficacy against the local tissue damaging activities of venoms [7]. Thus, there is a need to search for inhibitors and approaches that may be useful to complement conventional antivenom therapy.

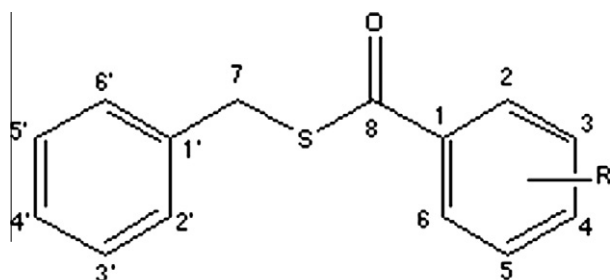
Thioester compounds present antiviral activity against HIV-1 virus [8,9] and also may act as intermediary metabolites of carboxylate-containing drugs, in fact, many steroidal anti-inflammatory agents may form S-acyl-coA thioesters *in vivo*. In general, S-acyl-coA and reduced glutathione GSH play an important role against free radicals and are emerging as potentially significant intermediates in the metabolism of acidic drugs. These thioesters may represent a latent drug form that may be reactivated *via* hydrolysis [10]. We synthesized 4-chlorothiobenzoic acid S-benzyl ester (I), 3-nitrothiobenzoic acid S-benzyl ester (II), 4-nitrothiobenzoic acid S-benzyl ester (III) and 4-methylthiobenzoic acid S-benzyl ester (IV) (Fig. 1).

These compounds have two aromatic rings joined by a flexible bridge, the –CO–S–CH₂– moiety. To the best of our knowledge, till now, there is not available information about inhibitory activity against PLA₂ by thioester compounds. Therefore, we tested the inhibitory ability of title compounds on enzymatic activity of a snake venom PLA₂. In addition, we performed a molecular docking study to suggest a mode of action of substituted thiobenzoic acid S-benzyl esters.

2. Experimental

2.1. General

Solvents were evaporated from solutions in a rotary evaporator Heidolph Laborota 4010 equipped with a ROTAVAP valve control.



Compound	R ₃	R ₄
I	H	Cl
II	NO ₂	H
III	H	NO ₂
IV	H	CH ₃

Fig. 1. Studied compounds: 4-chlorothiobenzoic acid S-benzyl ester (I), 3-nitrothiobenzoic acid S-benzyl ester (II), 4-nitrothiobenzoic acid S-benzyl ester (III) and 4-methylthiobenzoic acid S-benzyl ester (IV).

Melting points (m.p.) were recorded in a Netzsch DSC 200 PCPhox or an Electrothermal 9100 apparatus. The mass spectra were measured with a CG-MS Shimadzu QP-2010 spectrometer with a HP-5 column. Infrared spectra in KBr pellets have been measured between 4000 and 400 cm⁻¹ (4 cm⁻¹ resolution) with and FT-IR spectrometer Thermo-Nicolet IR200. NMR spectra were measured at 298 K on a Bruker DPX 200 spectrometer. The compounds were dissolved in CDCl₃. Chemical shifts, δ , are given in ppm relative to TMS ($\delta = 0$ ppm) and are referenced by using the residual undeuterated solvent signal. Coupling constants, *J*, are reported in Hz, multiplicities being marked as: singlet (s), doublet (d), triplet (t), double triplet (dt) of multiplet (m).

2.2. Syntheses

General procedure: The thiobenzoic acid S-benzyl esters were prepared by adapting a method previously reported by Henao Castañeda [11]. The respective aryl chloride (11.0 mmol) was dissolved in dry pyridine (2.0 mL), the resulting solution stirred mechanically at 20 °C and then, benzylthiol (10.0 mmol) was added in one step. The reaction mixture became immediately warmer and was kept at 20–22 °C under Argon atmosphere with stirring for 1 h. [12] After isolation, the crude product was purified by silica gel flash chromatography followed by crystallization, to obtain the compounds I–IV.

2.3. Spectroscopical characterization

4-Chloro-thiobenzoic acid S-benzyl ester (I): Colorless crystals; yield 95%; m.p. 52.6 °C (DSC). MS (EI) $m/z = 262$ [M]⁺. ¹H NMR (CDCl₃, 200 MHz, 25 °C): $\delta = 7.80$ (2H, dt, *J* = 8, 2 and <1 Hz, H2 and H6); 7.30 (2H, dt, *J* = 8, 2 and <1 Hz, H3 and H5); 7.30–7.10 (5H, m, C₆H₅); 4.29 (2H, s, CH₂) ppm; ¹³C NMR (CDCl₃, 62.98 MHz, 25 °C): $\delta = 190.1$ (C=O); 141.4 (C1'); 139.8 (C4); 131.9 (C1); 129.0 (C2 and C6); 128.9 (C3 and C5); 128.7 (C3' and C5'); 128.6 (C2' and C6'); 127.4 (C4'); 33.5 (CH₂) ppm.

3-Nitro-thiobenzoic acid S-benzyl ester (II): Colorless crystals; yield 95%; m.p. 47.6 °C (DSC). MS (EI) $m/z = 273$ [M]⁺. ¹H NMR (CDCl₃, 200 MHz, 25 °C): $\delta = 8.71$ (1H, t, *J* = 2 Hz, H2); 8.33 (1H, dt, *J* = 8 and 2 Hz, H4); 8.18 (1H, dt, *J* = 8 and 2 Hz, H6); 7.57 (1H, t, *J* = 8 Hz, H5); 7.30–7.10 (5H, m, C₆H₅); 4.29 (2H, s, CH₂) ppm; ¹³C NMR (CDCl₃, 62.98 MHz, 25 °C): $\delta = 189.3$ (C=O); 148.3 (C3); 138.0 (C1'); 136.6 (C1); 132.7 (C6); 132.7 (C5); 129.9 (C4); 128.7 (C3' and C5'); 127.6 (C2' and C6'); 127.6 (C4'); 122.2 (C2); 33.5 (CH₂) ppm.

4-nitro-thiobenzoic acid S-benzyl ester (III): Colorless crystals; yield 98%; m.p. 85.4–86.5 °C. MS (EI) $m/z = 273$ [M]⁺. ¹H NMR (CDCl₃, 200 MHz, 25 °C): $\delta = 8.20$ (2H, dt, *J* = 8, 2 and <1 Hz, H3 and H5); 8.00 (2H, dt, *J* = 8, 2 and <1 Hz, H2 and H6); 7.30–7.20 (5H, m, C₆H₅); 4.30 (2H, s, CH₂) ppm; ¹³C NMR (CDCl₃, 62.98 MHz, 25 °C): $\delta = 190.2$ (C=O); 151.0 (C4); 141.8 (C1'); 137.0 (C1); 129.4 (C2 and C6); 129.2 (C3' and C5'); 128.7 (C2' and C6'); 128.1 (C4'); 124.3 (C3 and C5); 34.3 (CH₂) ppm.

4-Methyl-thiobenzoic acid S-benzyl ester (IV): Colorless crystals; yield 95%, m.p. 43.5–44.1 °C MS (EI) $m/z = 242$ [M]⁺. ¹H NMR (CDCl₃, 200 MHz, 25 °C): $\delta = 7.93$ (2H, d, *J* = 8 Hz, H2 and H6); 7.29–7.46 (7H, m, H3 and H5; and C₆H₅); 4.37 (2H, s, CH₂); 2.45 (3H, s, CH₃) ppm; ¹³C NMR (CDCl₃, 62.98 MHz, 25 °C): $\delta = 190.8$ (C=O); 144.2 (C4); 137.6 (C1'); 134.2 (C1); 129.2 (C3 and C5); 128.9 (C3' and C5'); 128.6 (C2 and C6); 127.3 (C2' and C6'); 127.2 (C4'); 33.2 (CH₂); 21.6 (CH₃) ppm.

2.4. Toxin isolation

Crotalus durissus cumanensis venom was obtained from four specimens coming from Meta, in the south east region of Colombia,

and kept in captivity at the serpentarium of the Universidad de Antioquia (Medellín, Colombia). PLA₂ was purified by molecular exclusion chromatography on Sephadex G-75 and reverse-phase HPLC on C-18 column eluted at 1.0 mL/min with a gradient from 0% to 100% acetonitrile in 0.1% trifluoroacetic acid (v/v). Absorbance in effluent solution was recorded at wavelength of 280 nm [13].

2.5. Inhibition of phospholipase A2 activity using phosphatidylcholine as substrate

This activity was assayed according to the method reported by Dole [14], with titration of free fatty acids (FA) released from phosphatidylcholine (from dried egg yolk, Sigma) suspended in 1% Triton X-100, 0.1 M Tris-HCl, 0.01 M CaCl₂, pH 8.5 buffer, using 20 µg/10 µL of PLA₂. The time of reaction was 15 min at 37 °C. The amount of protein was selected from the linear region of activity curves. For inhibition experiments, 2 µM of each compound were pre-incubated for 30 min at 37 °C before PLA₂ activity determination. The results are indicated as inhibition percentage, where 100% is the activity induced by PLA₂ alone.

2.6. Inhibition of phospholipase A2 activity using 4-nitro-3-octanoyloxybenzoic acid (4N3OBA) as substrate

The measurements of enzymatic activity using the linear substrate 4N3OBA were performed according to the method described by Holzer and Mackessy [15] and adapted for a 96-well ELISA plate. The standard assay contained 200 µL of buffer (10 mM Tris-HCl, 10 mM CaCl₂, 100 mM NaCl, pH 8.0), 20 µL of 10 mM of substrate (4N3OBA), 20 µL of sample (20 µg PLA₂ or 20 µg PLA₂ + 50 µM of each compound) and 20 µL of water. The negative control was only buffer. The inhibitory effect of the compounds **I–IV** on PLA₂ activity was determined through co-incubation of the enzyme with each compound for 30 min at 37 °C. After the incubation period, the sample was added to the assay and the reaction was monitored at 425 nm for 40 min (at 10 min intervals) at 37 °C. The quantity of chromophore released (4-nitro-3-hydroxy benzoic acid) was proportional to the enzymatic activity, and the initial velocity (V_0) was calculated considering the absorbance measured at 20 min.

2.7. Computational studies

Quantum chemical calculations were carried out with the GAUSSIAN 09 [16] program package, implemented on a personal computer. The geometric structures for the more stable conformers were calculated at the B3LYP/6-31+G(d,p) level of approximation and the same method was used to determine the vibration mode frequencies of the free molecules. Assignment of vibrational modes was obtained by visual inspection of displacement vectors using Gauss View 5 [17]. The potential energy curve around the dihedral angle $\delta C6'-C1'-C7-S$ was calculated for compounds **I–IV** employing the B3LYP/6-31+G(d,p) approximation with structure optimization for the torsion angle in steps of 30°. The calculations were performed for molecules in vacuum (gas phase) and therefore environmental effects were not considered. Some physicochemical properties of compounds (**I–IV**) were obtained from Molinspiration [18] and are showed in Table 1. Molecular docking was carried out on a personal computer using Autodock Vina [19]. The PLA₂ (PDB code 2QOG) from *Crotalus durissus terrificus* showed 57% homology in the N-terminal with the PLA₂ used on *in vitro* studies [13]. Protein was used without water molecules. The structure of the protein was prepared using the Protein Preparation module implemented in the Maestro program. First, hydrogen atoms were automatically added to each protein according to the chemical

nature of each amino acid, on the basis of the ionized form, expected in physiological condition. This module also controls the atomic charges assignment. Second, each 3D structure of the protein was relaxed through constrained local minimization, using the OPLS force fields in order to remove possible structural mismatches due to the automatic procedure employed to add the hydrogen atoms. When necessary, bonds, bond orders, hybridizations, and hydrogen atoms were added, charges were assigned (a formal charge of +2 for Ca ion) and flexible torsions of ligands were detected. The α -carbon of His48 was used as center of the grid ($X = 44.981$, $Y = 27.889$ and $Z = 46.392$), whose size was 24 \AA^3 . Exhaustiveness = 20. Then, the ligand poses with best affinity were chosen, and a visual inspection of the interactions at the active site was performed and recorded. MMV [20] was used to generate docking images.

3. Results and discussion

3.1. Vibrational analysis

Compounds **I**, **II**, **III** and **IV** present 78, 84, 84 and 87 normal modes of vibration, respectively. Normal modes from the benzyl ring were quite similar in the four compounds, and the normal modes originated in the benzoate ring showed some differences due to the different substitution pattern. Vibrational frequencies calculated at B3LYP/6-31+G(d,p) were scaled by 0.964 [21]. The spectral position of the C=O carbonyl experimental bands appeared at 1664, 1653, 1643 and 1653 cm^{-1} ; while calculated $\nu_{C=O}$ bands appeared at 1661, 1663, 1662 and 1660 cm^{-1} for compounds **I–IV**, respectively. The C8-S stretching vibration was assigned to the bands at 920, 916, 927 and 908 cm^{-1} ; and the calculated bands appeared at 892, 925, 897 and 870 cm^{-1} , for compounds **I–IV** respectively. These data are in agreement with previous studies of organic thioester compounds [22].

3.2. Biological, conformational and docking analysis

Phospholipases A₂-induced myotoxicity occurs in two clinical patterns: local and systemic myotoxicity [21]. The action of these enzymes may result in irreversible lesions, which in addition to edema, hemorrhage and blistering may lead to amputation of the affected limb [23–25]. Moreover, it has been demonstrated that antivenoms, the current therapy for snakebite, generally have a limited efficacy against the local tissue damaging activities of venoms [26]. In addition, enzymatic activity of the PLA₂s is a key step on the induction of myonecrosis, inflammation and neurotoxicity induced by PLA₂ [24,27,28]. Thus, it is necessary to search for additional inhibitors and approaches that may be useful counterparts to conventional antivenom therapy. In this direction, we assayed the ability of the compounds **I–IV** to inhibit the enzymatic activity of a venom PLA₂. As described in Table 2, we used two substrates, in both cases compound **II** showed the best inhibitory ability; whereas, compounds **I** and **III** displayed comparable inhibition

Table 1
Physicochemical properties and ligand-PLA₂ affinity.

Compound	Affinity (kJ/mol) ^a	Molecular weight (Da) ^b	Number of HB acceptors ^b	Number of HB donors ^b	LogP ^b
I	-30.5	262.8	1	0	4.58
II	-32.6	273.3	4	0	3.84
III	-30.5	273.3	4	0	3.86
IV	-31.8	242.3	1	0	4.35

^a Calculated with Autodock Vina.

^b Calculated using Molinspiration.

Table 2
Inhibition of PLA₂ activity by compounds I–IV.

Compound	Phosphatidylcholine as substrate ^a	4N3OBA as substrate ^b
I	45.18 ± 8.16	51.99 ± 1.55
II	74.89 ± 9.10	69.91 ± 1.38
III	54.21 ± 5.54	51.98 ± 2.89
IV	35.66 ± 2.32	30.75 ± 5.61

^a Assay using the aggregated substrate phosphatidylcholine, values are mean ± SEM of inhibition percentage. PLA₂ activity of the enzyme without any compound was taken as 100% of activity, *n* = 4.

^b Assay using the monodisperse substrate 4-nitro-3-octanoyloxybenzoic acid, values are mean ± SEM of inhibition percentage. PLA₂ activity of the enzyme without any compound was taken as 100% of activity, *n* = 4.

percentages and compound IV exhibited the lowest inhibition of the PLA₂ activity. Moreover, compounds I, III and IV showed statistical differences with respect to compound II in their inhibitory capacity.

The enzymatic activity of a PLA₂ depends on three principal factors (a) the integrity of the active site (residues His48, Asp49, Tyr52, Asp99) (b) coordination of Ca²⁺ (residues Tyr28, Gly30, Gly32 and Asp49) (c) the adsorption of the enzyme onto the lipid-water interface of the phospholipids membrane bilayer (interfacial binding surface) [5]. In order to suggest a mode of action of thiobenzoic acid *S*-benzyl esters, we performed a molecular docking study. The results of this computational approach suggest that compounds I–IV could interact with amino acids at the active site and other regions of PLA₂. All compounds showed an H-bonding interaction with His48 of the enzyme (Fig. 2a–d). This interaction would impede normal catalysis cycle, because PLA₂ general basic catalysis mechanism implies water activation by His48 for the subsequent nucleophilic attack of sn2 ligation of the glycerophospholipids that will be hydrolyzed [5]. Additionally, thiobenzoic acid *S*-benzyl esters displayed important Van der Waals interactions with Leu2, Asp49 and Lys69 residues. Also, the rings of compounds I–IV exhibited π - π stacking interaction with Tyr52 (active site), Phe5 (hydrophobic channel) and Trp31 (interfacial binding

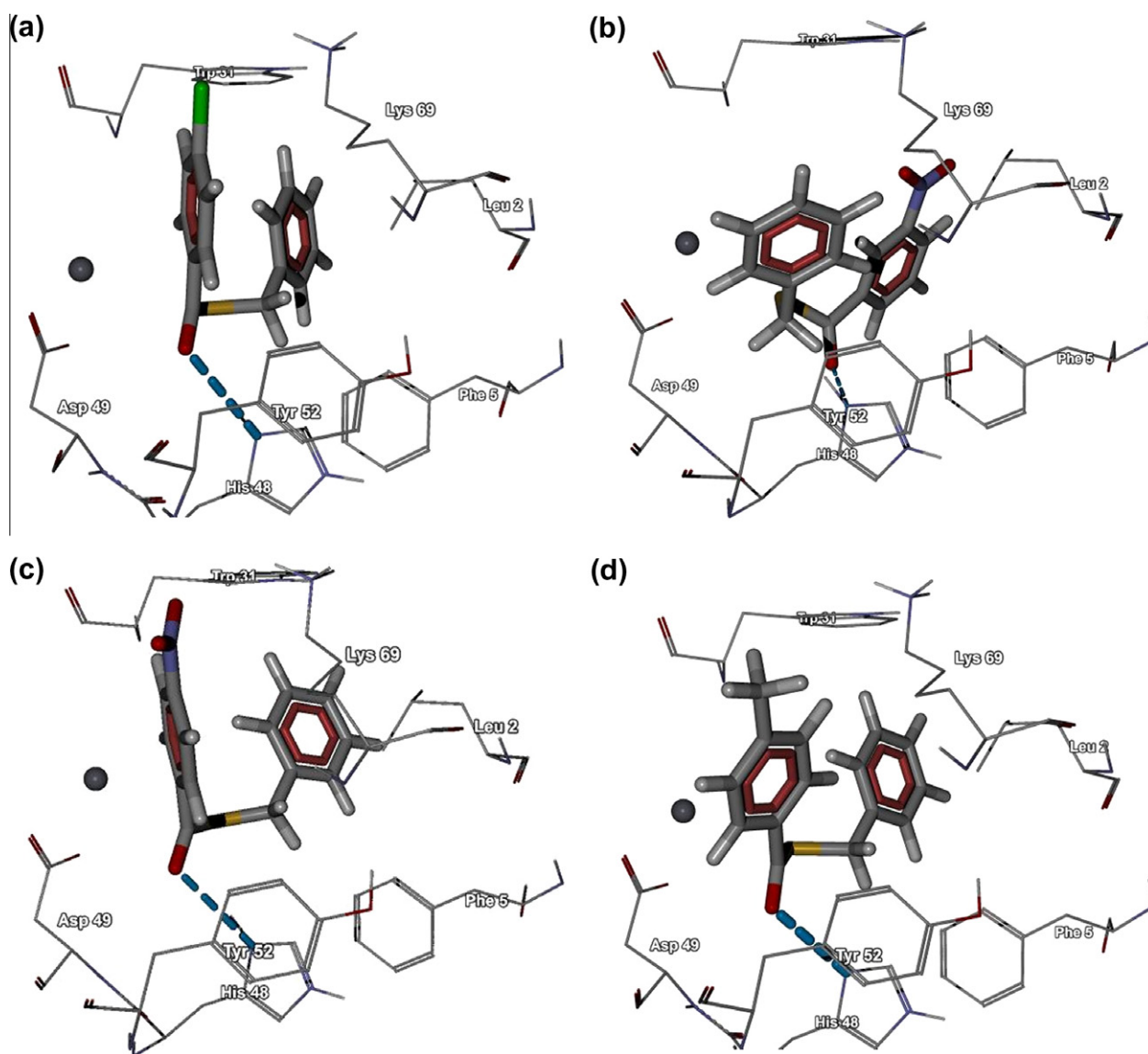


Fig. 2. PLA₂ binding site with main residues and docked conformation of (a) 4-chlorothiobenzoic acid *S*-benzyl ester (I), (b) 3-nitrothiobenzoic acid *S*-benzyl ester (II), (c) 4-nitrothiobenzoic acid *S*-benzyl ester (III) and (d) 4-methylthiobenzoic acid *S*-benzyl ester (IV). Gray sphere represents Ca²⁺. Dotted blue line represents a hydrogen bond. (For interpretation of the references to color in this figure legend, the reader is referred to the web version of this article.)

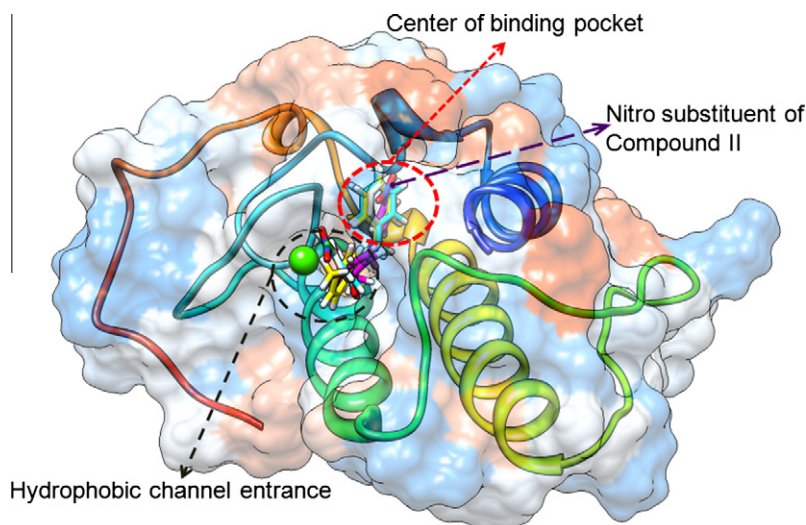


Fig. 3. Orientation of compounds I–V in the binding site of the PLA₂. Green sphere represents Ca²⁺. Dotted red circle shows the center of the binding pocket (active site of the enzyme). Dotted black circle displays the hydrophobic channel entrance. Note that compound II has the nitro substituent in the center of the binding pocket. (For interpretation of the references to color in this figure legend, the reader is referred to the web version of this article.)

surface). These weak interactions could stabilize the binding of each compound to the enzyme, and they could block the binding of the substrate to the active site of the PLA₂. The affinity of all compounds were very similar, however, compound II showed the best affinity by the PLA₂ (Table 1). Compounds I, III and IV showed the same orientation at the binding pocket of the enzyme, with benzyl ring placed into the center of the binding pocket of the toxin; as, in compound II, this ring was positioned in the hydrophobic channel entrance and the benzoate ring was located into the center of the protein cavity. (Fig. 3) This particular orientation could be influenced by the –CH₂–S–C(O) moiety, that also played an important role in the configuration of the title compounds in the active site of the PLA₂. After docking study, the dihedral angle $\delta C6'-C1'-C7-S$ for compounds I, II, III and IV in the lowest energy poses were 111.29°, 103.37°, 128.46° and 131.41°; and the values for the torsion angle $\delta O-C8-S-C7$ were 100.68°, 63.37°, 107.04° and 91.64°, respectively (Fig. 4). The difference in the $\delta O-C8-S-C7$ torsion angle of compound II in the active complex could be due to the different orientation in the active site respect to the other compounds.

Furthermore, compounds I–IV were promising, because they complied the Lipinski rules (molecular mass less than 500,

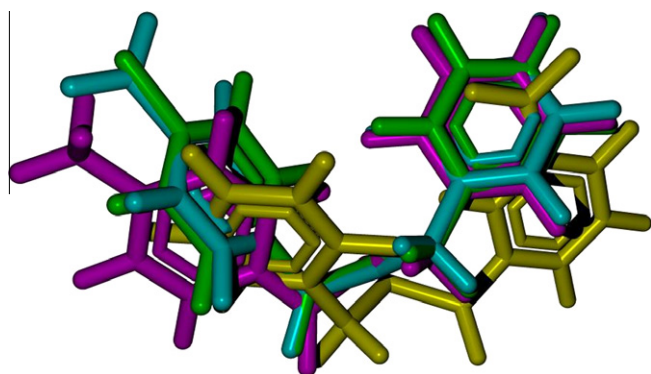


Fig. 4. Docked conformation of compounds I–IV in the lowest energy pose. Compound I: green; Compound II: yellow; Compound III: cyan; and Compound IV: magenta. Note differences in the dihedral angle C6'–C1'–C7–S. (For interpretation of the references to color in this figure legend, the reader is referred to the web version of this article.)

calculated log P less than 5, less than 10 hydrogen bond acceptor groups, less than five hydrogen bond donor groups), that would predict if a molecule was likely to be orally bioavailable [29] (see Table 1).

The thiobenzoic acid S-benzyl esters (I–IV) showed synperiplanar configuration around the dihedral angle ($\delta O-C8-S-C7$) with values within 4.30° and 3.59°. These values are in agreement with those found for organic thioester compounds [22,30]. The potential energy curves for the dihedral angle $\delta C6'-C1'-C7-S$ calculated with B3LYP/6-31+G(d,p) approximation are depicted in Fig. 5 and the minimum energy has been found at 90°. For the optimized conformations with B3LYP/6-31+G(d,p) values of 91.43°, 90.61°, 91.09° and 92.57° were found for compounds I, II, III and IV respectively, with a configuration of the benzyl ring in almost a perpendicular position with respect to the sulfenyl carbonyl function. Moreover, the torsion angle $\delta C8-S-C7-C1'$ completed the description of the central bridge between both aromatic rings; in the DFT calculations (molecules in vacuum) showed values of 94.78° (I), 94.17°

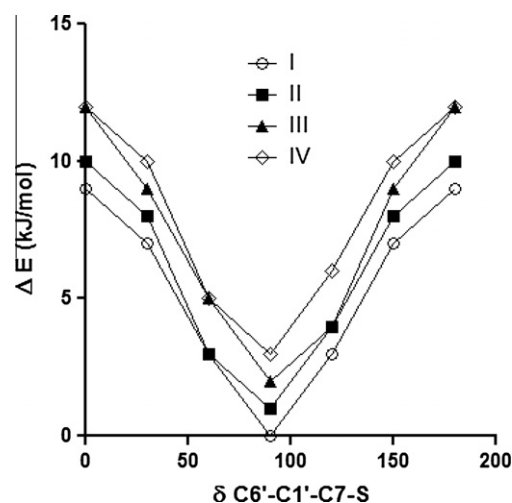


Fig. 5. Potential energy curve for compounds I, II, III, IV as a function of the C6'–C1'–C7–S torsion angle, calculated with the B3LYP/6-31+G(d,p) approximation. The curves have been shifted by 1, 2, and 3 kJ/mol for compounds I, II, III and IV respectively. (For interpretation of the references to color in this figure legend, the reader is referred to the web version of this article.)

(II), 94.00 (III) and 95.60 (IV) and the values for the compounds in the complex were 133.05°, 121.71°, 131.34° and 139.93° for compounds I, II, III and IV, respectively. Optimized geometrical parameters of thiobenzoic acid *S*-benzyl esters I–IV are included as [Supplementary material](#).

4. Conclusions

Thiobenzoic acid *S*-benzyl esters showed good inhibition ability on enzymatic activity of a venom PLA₂, with percentage of inhibition between 35.66% and 74.89%, with an average inhibition of 52.49%. Molecular docking study suggested the binding of thioesters to the active site of the enzyme. This interaction could explain the inhibition of enzymatic activity, by blocking the normal progression of the catalytic cycle and by impeding the normal attachment of the substrate to active site of the PLA₂. Further *in vivo* studies are needed to confirm inhibitory capacity of these compounds on toxic effects induced by this toxin. In addition, a large set of thioester compounds could be tested in order to evaluate their potency to neutralize these toxins.

Acknowledgements

JAPJ and ICHC acknowledge Programa de Sostenibilidad 2011 (Universidad de Antioquia) and Rodrigo Ochoa by his general technical help.

ICHC specially acknowledge DAAD, for a fellowship and Prof. Dr. Nils Metzler-Nolte for his support.

JLJ acknowledge the WUS organization (Word University Service, Deutsches Komitee e.V., APA Programm, Wiesbaden, Germany), for the provision of an FT-IR 200 equipment and the DAAD for the grant provided for the purchase of a rotary evaporator equipment.

Appendix A. Supplementary material

Supplementary data associated with this article can be found, in the online version, at <http://dx.doi.org/10.1016/j.molstruc.2012.06.031>.

References

- [1] F.S. Markland Jr., *Drugs* 54 (Suppl. 3) (1997) 1.
- [2] D.A. Six, E.A. Dennis, *Biochim. Biophys. Acta* 1488 (1–2) (2000) 1.
- [3] R.M. Kini, *Toxicol.* 42 (8) (2003) 827.
- [4] C. Bon, *Toxicol.* 34 (2) (1996) 142.
- [5] O.G. Berg, M.H. Gelb, M.D. Tsai, M.K. Jain, *Chem. Rev.* 101 (2001) 2613.
- [6] M. Murakami, T. Kudo, *Biol. Pharm. Bull.* 27 (8) (2004) 1158.
- [7] J.M. Gutiérrez, G. León, G. Rojas, B. Lomonte, A. Rucavado, F. Chaves, *Toxicol.* 36 (11) (1998) 1529.
- [8] P. Srivastava, M. Schito, R.J. Fattah, T. Hara, T. Hartman, R.W. Buckheit Jr., J.A. Turpin, J.K. Inman, E. Apella, *Bioorg. Med. Chem.* 12 (2004) 6437.
- [9] Y. Song, A. Goel, V. Basrur, *Bioorg. Med. Chem.* 10 (2002) 1263.
- [10] C. Ibarra, M.P. Grillo, M. Lo Bello, M. Nucetelly, T. Bammler, W.M. Atkins, *Arch. Biochem. Biophys.* 414 (2003) 303.
- [11] I.C. Henao Castañeda, PhD-Thesis, Facultad de Ciencias Exactas, Universidad Nacional de La Plata, La Plata, República Argentina.
- [12] J.L. Jios, S.I. Kirin, T. Weyhermüller, N. Metzler-Nolte, C.O. Della Védova, *J. Mol. Struct.* 825 (1–3) (2006) 53.
- [13] J.A. Pereañez, V. Núñez, S. Huancahuire-Vega, S. Marangoni, L.A. Ponce-Soto, *Toxicol.* 53 (5) (2009) 534.
- [14] V.P. Dole, *J. Clin. Invest.* 35 (2) (1956) 150.
- [15] M. Holzer, S.P. Mackessy, *Toxicol.* 34 (10) (1996) 1149.
- [16] M.J. Frisch, G.W. Trucks, H.B. Schlegel, G.E. Scuseria, M.A. Robb, J.R. Cheeseman, Gaussian 09, Revision B.01, Gaussian, Inc., Wallingford CT, 2010.
- [17] R. Dennington, T. Keith, J. Millam, GaussView, Version 5, Semicem Inc., Shawnee Mission KS, 2009.
- [18] <http://www.molinspiration.com/cgi-bin/properties>, 2012.
- [19] O. Trott, A.J. Olson, *J. Comput. Chem.* 31 (2010) 455.
- [20] Molegro Molecular Viewer 2.2.0. www.molegro.com, 2012.
- [21] www.cccbdb.nist.gov, 2012.
- [22] I.C. Henao Castañeda, J.L. Jios, O.E. Piro, G.E. Tobón, C.O. Della Védova, *J. Mol. Struct.* 842 (2007) 46.
- [23] C. Bon, M. Goffon (Eds.), *Envenomings and Their Treatments*, Fondation Marcel Merieux, Lyon, 1996 (Chapter 1).
- [24] J.M. Gutiérrez, C. Ownby, *Toxicol.* 42 (2003) 915.
- [25] V. Núñez, V. Castro, R. Murillo, L.A. Ponce-Soto, I. Merfort, B. Lomonte, *Phytochemistry* 66 (2005) 1017.
- [26] J.M. Gutiérrez, G. León, G. Rojas, B. Lomonte, A. Rucavado, F. Chaves, *Toxicol.* 36 (1) (1998) 529.
- [27] C.F. Teixeira, E.C. Landucci, E. Antunes, M. Chacur, Y. Cury, *Toxicol.* 42 (8) (2003) 947.
- [28] C. Montecucco, J.M. Gutiérrez, B. Lomonte, *Cell. Mol. Life. Sci.* 65 (18) (2008) 2897.
- [29] C.A. Lipinski, F. Lombardo, B.W. Dominy, P.J. Freney, *Adv. Drug. Deliv. Rev.* 23 (1997) 3.
- [30] I.C. Henao Castañeda, C.O. Della Védova, O.E. Piro, N. Metzler-Nolte, J.L. Jios, *Polyhedron* 29 (2010) 827.